UC Irvine
UC Irvine Previously Published Works

Title

Engineered drug-protein nanoparticle complexes for folate receptor targeting

Permalink

https://escholarship.org/uc/item/844259tq

Authors

Ren, Dongmei
Kratz, Felix
Wang, Szu-Wen

Publication Date

2014-08-01

DOI

10.1016/j.bej.2013.09.008

Peer reviewed

Engineered drug-protein nanoparticle complexes for folate receptor targeting

Dongmei Ren[1], **Felix Kratz**[2], and **Szu-Wen Wang**[1],[*]

[1] Department of Chemical Engineering and Materials Science University of California, 916 Engineering Tower, Irvine, CA 92697-2575, USA

[2] Tumor Biology Center, Division of Macromolecular Prodrugs Breisacher Strasse 117, D-79106 Freiburg, Germany

Abstract

Nanomaterials that are used in therapeutic applications need a high degree of uniformity and functionality which can be difficult to attain. One strategy for fabrication is to utilize the biological precision afforded by recombinant synthesis. Through protein engineering, we have produced ~27-nm dodecahedral protein nanoparticles using the thermostable E2 subunit of pyruvate dehydrogenase as a scaffold and added optical imaging, drug delivery, and tumor targeting capabilities. Cysteines in the internal cavity of the engineered caged protein scaffold (E2 variant D381C) were conjugated with maleimide-bearing Alexa Fluor 532 (AF532) and doxorubicin (DOX). The external surface was functionalized with polyethylene glycol (PEG) alone or with the tumor-targeting ligand folic acid (FA) through a PEG linker. The resulting bi-functional nanoparticles remained intact and correctly assembled. The uptake of FA-displaying nanoparticles (D381C-AF532-PEG-FA) by cells overexpressing the folate receptor was approximately six times greater than of non-targeting nanoparticles (D381C-AF532-PEG) and was confirmed to be FA-specific. Nanoparticles containing DOX were all cytotoxic in the low micromolar range. To our knowledge, this work is the first time that acid-labile drug release and folate receptor targeting have been simultaneously integrated onto recombinant protein nanoparticles, and it demonstrates the potential of using biofabrication strategies to generate functional nanomaterials.

Keywords

biosynthesis; protein; targeted drug delivery; folic acid; biomedical; biomimetics; bionanotechnology

[*]Corresponding author wangsw@uci.edu Phone: 949-824-2383 Fax: 949-824-2541.

1. INTRODUCTION

Functional nanoparticles have promising potential for broad applicability, but many challenges exist in chemically synthesizing materials at such small sizes. In contrast, natural biological systems have been highly successful in this endeavor, and therefore nature-inspired macromolecular architectures can be used as the basis upon which new types of materials are made [1, 2]. In this work, we demonstrate that the detailed control which genetic engineering provides in defining the polymeric architecture of proteins can be coupled with synthetic strategies to introduce new multiple functionalities into a nanoparticle scaffold. This approach enables the creation of defined and uniform nanoparticles that are potentially applicable for drug delivery.

Our biomimetic scaffold is a 25-nm virus-like protein nanoparticle modeled from the E2 subunit of a pyruvate dehydrogenase multienzyme complex. It is composed of 60 identical subunits, contains 12 openings which lead to a hollow internal cavity, and is stable up to ~80 °C [3, 4]. Unlike other protein-based nanoparticles, it is non-viral in origin. Our research has demonstrated that the internal, external, and subunit-subunit interfaces of the E2 protein scaffold can be individually engineered for various capabilities such as drug encapsulation, modulation of immune response, and pH-dependent disassembly, respectively [5-8].

The size of this protein assembly has a decisive relevance for intracellular drug delivery applications. Others have reported that the optimal size range for cellular particle uptake is approximately 25-75 nm [9, 10], and particles of this size also accumulate in tumor tissues due to the enhanced permeability and retention effect [11, 12]. Tumor targeting can also be actively implemented by attaching ligands to nanoparticles that target tumor-associated receptors. This approach utilizes the over-expression of receptors on the surface of tumor cells relative to normal cells [13, 14] and have included folate, transferrin, and integrin binding receptors [13-15].

Of these, the folate receptor (FR) has been extensively investigated and widely used. FR is a membrane glycoprotein with a molecular weight of 38-40 kDa, and it is overexpressed in various tumors such as ovarian, brain, lung, and breast cancers [16-19]. The corresponding targeting ligand, folic acid (FA, vitamin B9), is involved in one-carbon metabolic transfer reactions, is critical in nucleotide synthesis and the viability of proliferating cells, and exhibits a high affinity for FR ($K_d \sim 10^{-10}$ M) [17, 18]. FA can be coupled to anti-tumor drugs directly [18, 20] or to various macromolecular delivery systems, including liposomes, micelles, polymers, or inorganic particles [16, 17, 21, 22].

To our knowledge, genetically engineered protein-based nanoparticles combining the dual functionalities of acid-responsive drug release and FA targeting have not yet been reported. In this work, we fabricate an E2 protein scaffold in a recombinant *E. coli* system and further extend the utility of these nanoparticles by simultaneously incorporating imaging/targeting and drug/targeting abilities through chemical conjugation. The fluorescent molecule Alexa Fluor 532 (AF532) and a derivative of the anti-cancer drug doxorubicin (DOX), the (6-maleimidocaproyl)hydrazone derivative of doxorubicin (DOXO-EMCH), which both contain a thiol-reactive maleimide group (see Figure 1), were coupled to the internal cavity

of the E2 variant D381C [5]. Attachment of FA to the outer nanoparticle surface was achieved through a polyethylene glycol (PEG) linker. PEGylation is a typical strategy to modulate the immune response and increase the nanoparticle circulation time *in vivo* [23], and our prior work showed that PEGylation of the E2 surface significantly decreased the nonspecific cellular uptake [8]. We examine cellular uptake of our functionalized protein-based nanoparticles in cell lines expressing high and low amounts of FR, and we measured the cytotoxicity of these particles in cancer cells. Our results demonstrate the broad potential of utilizing biomimetic structures and biofabrication strategies as viable approaches to extend nanotechnology applications.

2. MATERIALS AND METHODS

2.1 Materials

Sodium chloride (NaCl), sodium dodecyl sulfate (SDS), hydrochloric acid (HCl), sodium phosphate dibasic, sodium phosphate monobasic, *N,N*-dimethylformamide (DMF), and magnesium chloride hexahydrate ($MgCl_2 \cdot 6H_2O$) were supplied by EMD. Alexa Fluor 532 C_5 maleimide (AF532) and Hoechst 33342 were obtained from Invitrogen. Dimethyl sulfoxide (DMSO) and cysteine·HCl were purchased from Thermo Scientific. Tris(2-carboxyethyl) phosphine hydrochloride (TCEP) was from Pierce. Tris base, bovine serum albumin, potassium phosphate monobasic, and potassium phosphate dibasic were from Fisher Scientific. A heterobifunctional polyethylene glycol (PEG) linker (2000 Da) with folic acid (FA) and N-hydroxysuccinimide (NHS) at each respective end (FA-PEG-NHS) and a PEG linker (2000 Da) functionalized with maleimide and NHS at each respective end (Mal-PEG-NHS) were obtained from Nanocs. The (6-maleinimidocaproyl) hydrazone derivative of doxorubicin (DOXO-EMCH) was synthesized and characterized as previously described [24] and doxorubicin hydrochloride (DOX) was from Yic-Vic. DOX and DOXO-EMCH were dissolved in 10 mM sodium phosphate (pH 5.8) and used within 30 minutes. Dulbecco's Modified Eagle's Medium (DMEM), DMEM without folic acid, and CelLytic M cell lysis reagent were purchased from Sigma-Aldrich. PBS was from MP Biomedicals. Fetal bovine serum (FBS), L-glutamine, and penicillin-streptomycin were obtained from Mediatech. Folic acid was from Fisher BioReagents. Non-fat dry milk was from LabScientific. KB, A549, and HeLa cells were obtained from ATCC.

2.2 Protein expression and purification

The E2 protein scaffold consists of 60 identical subunits, with no surface-accessible cysteines on the native wild-type scaffold. To conjugate guest molecules into the hollow cavity of the E2 protein scaffold, the aspartic acid at position 381 of the E2 scaffold was mutated to cysteine, resulting in 60 thiols (one per subunit) in the internal surface of the nanocapsule (mutant designated as D381C) [3]. Guest molecules, such as the fluorescent marker AF532 and anticancer drug doxorubicin, can be conjugated to D381C through these thiols in a fast Michael addition [5].

Detailed experimental procedures for the mutagenesis, expression, and purification of D381C have been reported in previous studies [3, 5]. In summary, we performed site-directed mutagenesis, cloned the gene into the expression plasmid, and transformed the

plasmid into *E. coli* BL21(DE3). Cells induced to express protein nanoparticles were harvested and lysed. Protein nanoparticles were purified with a fast protein liquid chromatography (FPLC) system (ÄKTA, Amersham Biosciences) using Q Sepharose and Superose 6 PG columns.

2.3 Chemical functionalization of recombinant protein nanoparticles

The nanoparticles that were synthesized for this study and their abbreviations are summarized in Figure 2. Conjugation of AF532 to D381C (D381C-AF532) was performed following protocols similar to those previously described [5]. Purified protein scaffolds D381C were mixed with AF532 at a ratio of 1 subunit: 2.5 molecules at room temperature for 2 hrs, followed by 4 °C overnight incubation. Unbound AF532 were removed by desalting columns (Zeba, 40 kDa MWCO, Pierce) following the vendor protocol. Samples were loaded onto columns equilibrated with phosphate buffer and centrifuged. The unbound AF532 was retained in the resin while D381C-AF532 was recovered in the flow-through.

We conjugated polyethylene glycol (PEG) onto the external surface lysines of D381C-AF532. Briefly, FA-PEG-NHS and Mal-PEG-NHS were dissolved in DMSO under argon. D381C-AF532 was then mixed with FA-PEG-NHS or Mal-PEG-NHS at a ratio of 1 subunit: 5 PEG linkers at room temperature for 1 hr. Since the internal thiols are conjugated with AF532 and no other surface-accessible cysteines are present, Mal-PEG-NHS will only react with amines through the NHS ester. The unbound PEG linkers were removed by desalting columns. The functionalized protein scaffolds were designated D381C-AF532-PEG-FA and D381C-AF532-PEG-Mal, respectively.

To avoid reaction of unreacted maleimides on the PEG molecule during cellular assays, we capped the maleimide groups on D381C-AF532-PEG-Mal with thiols from free cysteines. Cysteines were mixed with TCEP at a molar ratio of 1 cysteine: 1 TCEP at room temperature for 30-45 minutes to prevent disulfide bonds formation. D381C-AF532-PEG-Mal was then mixed with the cysteines at a ratio of 1 subunit: 5 cysteine molecules at room temperature for 1 hr. Unreacted cysteines were removed by desalting columns. These protein nanoparticles were designated D381C-AF532-PEG.

To load the antitumor drug doxorubicin into E2 nanoparticles, we first coupled DOXO-EMCH to the empty D381C protein scaffold, as described in Ren *et al.* [5]. DOXO-EMCH contains a pH-sensitive hydrazone linker which releases doxorubicin (DOX) in acidic environments such as in the endosomes or lysosomes, and we have previously characterized this drug release from the D381C scaffold [5]. After drug conjugation within the internal E2 cavity, the addition of the folic acid (FA) targeting ligand and the amino acid-capped PEG to create D381C-DOX-PEG-FA and D381C-DOX-PEG, respectively, was performed (as described above for D381C-AF532-PEG-FA and D381C-AF532-PEG).

2.4 Characterization of functionalized protein nanoparticles

We quantified the number of AF532, DOX, and FA molecules conjugated per protein nanoparticle. Protein concentration was measured by Micro BCA (Pierce) using bovine serum albumin as a standard. AF532 and DOX concentrations were determined by

absorbance at 526 nm and 495 nm, respectively, using respective mass standard curves. The amount of FA attached to protein nanoparticles was calculated by absorbance at 358 nm (with a FA extinction coefficient of 15,760 M^{-1} cm^{-1} [25]), using D381C-AF532-PEG-Mal as the subtracted background.

We performed SDS-PAGE and Western blot to detect PEGylated proteins and conjugated FA. Protein nanoparticles were run on a 12% Tris-HCl SDS-PAGE gel and stained. For detection of FA, the protein gel was transferred to a positively charged nylon membrane (Roche Diagnostic). Folic acid on D381C-AF532-PEG-FA was detected by mouse anti-folic acid monoclonal primary antibody (Sigma-Aldrich) diluted 2000 times in blocking solution (0.5% non-fat dry milk in 20 mM Tris-HCl, 500 mM NaCl buffer, pH 7.5). Rabbit anti-mouse IgG conjugated with alkaline phosphatase (Invitrogen, Life Technologies), was diluted 1000-fold in blocking solution and used as secondary antibody. Western blot was developed in 2% NBT/BCIP (Roche Diagnostics) diluted in buffer containing 100 mM Tris, 50 mM $MgCl_2$, 100 mM NaCl (pH 9.5). Molecular weight protein standards for SDS-PAGE and Western blots were from Novogen and Bio-Rad, respectively.

The hydrodynamic diameters of protein nanoparticles were determined by dynamic light scattering (DLS) using a Zetasizer Nano ZS (Malvern Instruments). The measurements were performed on 0.06-0.1 mg/mL protein samples in phosphate buffer (defined here as 50 mM potassium phosphate, 100 mM NaCl, pH 7.4). Averages were obtained for n   3 measurements per batch, for at least two independent batches of functionalized nanoparticles.

We confirmed the secondary structure of the synthesized protein scaffolds by far-UV circular dichroism (CD) using a Jasco 810 spectropolarimeter. Protein samples at 0.06 mg/mL in phosphate buffer were scanned from 200 nm to 260 nm at a rate of 10 nm/min in 0.1 cm pathlength quartz cells. Each spectrum was an average of three measurements.

2.5 Determination of folate receptor expression

The folate receptor (FR) on cell surfaces binds folic acid specifically. To select FR-positive and FR-negative cells, we examined the FR expression levels in three different carcinoma cell lines: KB, A549, and HeLa. The cells were cultured in DMEM medium supplemented with 10% fetal bovine serum, 1% L-glutamine, and 1% penicillin-streptomycin at 37°C in 5% CO_2 atmosphere. Cells were grown in tissue culture treated Petri dishes (BD Falcon) to near confluency, and lysed with CelLytic M cell lysis reagent following the vendor protocol for adherent cells. The soluble proteins extracted from the cells were run on a 12% SDS-PAGE, followed by Western blot detection. FR was detected using rabbit anti-FR (Santa Cruz Biotechnology) as the primary antibody, and goat anti-rabbit IgG-alkaline phosphatase (Millipore) as the secondary antibody, both diluted 500 times in blocking solution. The Western blots were developed in 2% NBT/BCIP solution.

2.6 Cellular uptake of protein nanoparticles conjugated with and without folic acid

Based on the FR expression levels, we selected cells expressing high levels (KB) and low levels (A549) of FR. Cells were then cultured in FA-free DMEM supplemented with 10% fetal bovine serum, 1% L-glutamine, and 1% penicillin-streptomycin (designated as "growth

medium") at 37°C in 5% CO_2 atmosphere. We seeded 1.3×10^5-1.5×10^5 cells per well into tissue culture treated 48-well plates (BD Falcon). After 20 hr incubation at 37°C, the growth medium was replaced with fresh growth medium containing D381C-AF532-PEG-FA or D381C-AF532-PEG (at equivalent concentrations of 0.046 μM protein and 2.8 μM AF532). The cells were incubated in protein solutions (samples) or growth media alone (control) at 37°C for 0.5 h. Cells were harvested, washed, and re-suspended in FACS buffer (1% bovine serum albumin, 0.2% sodium azide in PBS buffer). The fluorescence of AF532 in cells was detected by a BD Accuri C6 Flow Cytometer, and nanoparticle uptake data was analyzed by BD Accuri C6 software. Specifically, the histogram for the control cells (without nanoparticles, without fluorescence) was used as a reference to which each sample was compared. Cells with fluorescence intensities higher than the control cells were considered positive cells with AF532 fluorescence. The percentage of cell uptake was defined as the number of positive (fluorescent) cells divided by the total number of cells measured in the sample (typically, ~50,000 cells per sample). We did not quantify uptake using nanoparticles containing DOX (D381C-DOX-PEG-FA, D381C-DOX-PEG) because of the potential cytotoxicity of DOX on the cells (see section 3.6).

2.7 Inhibition assays with free folic acid

KB and A549 cells (1.3×10^5- 1.5×10^5 cells per well) were seeded into tissue culture treated 48-well plates and incubated at 37°C for 16 hrs. Folic acid saturates on FR-expressing cancer cells in less than 1 hr, with this saturation plateau remaining constant for up to at least 6 hrs [26]. Therefore, to saturate FR, the cells were pre-incubated in fresh growth medium containing 1 mM FA for 2-3 hrs. Control cells were cultivated in growth medium only. After incubation, the medium was replaced by new medium which contained D381C-AF532-PEG-FA or D381C-AF532-PEG (at equivalent concentrations of 0.046 μM protein and 2.8 μM AF532), and cells were incubated for 0.5 h at 37°C. Cells were then harvested and analyzed by flow cytometry as described in section 2.6.

2.8 Imaging of protein nanoparticle internalization by cells using confocal laser scanning microscopy (CLSM)

KB cells (40,000 cells per well) were seeded in an 8-well Lab-Tek chambered coverglass (Thermo Scientific Nunc) and incubated at 37°C for 20 hrs. The growth medium was then replaced with fresh growth medium containing D381C-AF532-PEG-FA or D381C-AF532-PEG (at equivalent concentrations of 0.038 μM protein and 2.6 μM AF532) and incubated with the cells at 37°C for 20 minutes. Cells were then washed and incubated with 0.4 μg/mL Hochest 33342 in growth medium for 40 minutes to stain the nucleus. After staining, the cells were washed and imaged in PBS with a Zeiss LSM 510 confocal microscope. Imaging parameters included excitation/emission filter wavelengths of 543 nm/565-615 nm bandpass for AF532 and 800 nm 2-photon excitation (equivalent 400 nm single photon excitation)/ 435-485 nm bandpass for Hoechst 33342.

2.9 Cytotoxicity of D381C-DOX-PEG-FA and D381C-DOX-PEG

To evaluate cytotoxicity of D381C-DOX-PEG-FA and D381C-DOX-PEG in cell lines expressing high and low concentrations of FR, we performed MTT assays based on previously described protocols [27]. KB and A549 cells were deposited into tissue culture

treated 96-well plates (BD Falcon) at 5000 cells per well, grown overnight in growth medium, and then incubated for 48 hr with growth medium containing D381C-DOX-PEG-FA, D381C-DOX-PEG, D381C-DOX, or free DOX at final equivalent DOX concentrations of 0.001, 0.004, 0.02, 0.1, 0.3, 1, 3, and 8 μM. Cell viability was measured by the MTT assay. To calculate IC_{50} values, data for percent cell viability versus DOX concentrations was fitted to a 4-parameter Hill model using KaleidaGraph (v. 4.1, Synergy Software).

3. RESULTS AND DISCUSSION

3.1 Protein nanoparticles can simultaneously display functional groups on both the internal and external surfaces

Guest molecules in the internal cavity—The E2 nanoparticle consists of 60 identical subunits which self-assemble into a hollow dodecahedron. Introduction of 60 cysteines to the internal surface of these nanoparticles via genetic engineering (variant D381C) enables loading of guest molecules through the cysteine thiol groups. As described previously [3, 5], we can conjugate AF532 and doxorubicin (DOX) to the internal cavity of the D381C nanoparticles using maleimide conjugation chemistry.

For the imaging molecule AF532, an average of 73.6 ± 11.7, 72.3 ± 12.9, and 68.0 ± 4.9 AF532 molecules were attached to each protein nanoparticle D381C-AF532-PEG-FA, D381C-AF532-PEG, and D381C-AF532, respectively (Table 1). To utilize the targeted nanoparticles as a drug delivery vehicle, the antitumor drug DOX was loaded into the hollow cavity of the D381C nanoparticles at a DOX-to-nanoparticle ratio of 82.2 ± 5.1, 80.1 ± 3.0, and 99.3 ± 10.1 for D381C-DOX-PEG-FA, D381C-DOX-PEG and D381C-DOX, respectively (Table 1). As previously described, although the theoretical maximum number of AF532 or DOX is 60 molecules per scaffold, these values are larger due to non-specific binding, and they are consistent with previous results [5].

Functionalized ligands on the external surface—In this study, we utilize FA-PEG-NHS and Mal-PEG-NHS to attach to the primary amines of lysines on the surface of D381C-AF532 and D381C-DOX. More than one-third of the 1260 lysines on the E2 capsule are surface-accessible on the external surface [8]. We measured an average of 35.1 ± 6.3 and 27.9 ± 0.4 FA molecules per D381C-AF532-PEG-FA and D381C-DOX-PEG-FA nanoparticle, respectively (Table 1). Others have reported that a range of 20-60 FA molecules per nanoparticle [28] and as few as 1-2 FA per protein [29] is sufficient for cellular uptake by cells expressing the folate receptor (FR). Therefore, we are well within the minimum range of folate ligands for FR targeting.

We further confirmed successful surface conjugation by SDS-PAGE (Figure 3A) and Western blot (Figure 3B). Based on the measurement of ~30 FA conjugated per nanoparticle (Table 1), which is equivalent to approximately half the subunits in one nanoparticle, we expected to detect two main populations (PEGylated and unPEGylated) on an SDS-PAGE gel for each of the following samples: D381C-AF532-PEG, D381C-AF532-PEG-FA, D381C-DOX-PEG, and D381C-DOX-PEG-FA. Compared to D381C-AF532 and D381C-DOX, which show a single band near 29 kDa (as expected), we indeed observed additional bands in the PEGylated samples (Figure 3A). Although these bands for PEGylated protein

run at higher molecular weights than expected, this observation is consistent with other studies and has been hypothesized to be due to the complex interaction between PEG chains and SDS micelles [28, 30].

A Western blot of the protein nanoparticles confirms the conjugation of the FA ligands (Figure 3B). As expected, FA is detected by the anti-FA antibody in D381C-AF532-PEG-FA, while no bands are observed in D381C-AF532-PEG or D381C-AF532. In addition, no bands are observed near 29 kDa in the lane for D381C-AF532-PEG-FA, which would be the population of the subunits not functionalized with FA. When compared to the SDS-PAGE gel (Figure 3A), the FA bands in D381C-AF532-PEG-FA are consistent with the regions attributed to PEGylated protein.

3.2 Functionalized protein nanoparticles remain structurally intact after modification

The intact assembly of D381C nanoparticles after functionalization with guest molecules (internally) and targeting ligand (externally) was verified by dynamic light scattering (DLS) and circular dichroism (CD). Unfunctionalized D381C has a hydrodynamic diameter of ~27 nm [3] **(Figure 3C)**. The diameters of the functionalized particles average ~35 - 45 nm and are within the range for optimal nanoparticle uptake by cells [9, 10]. (See Table 1 for size summary and Figure 3C for representative DLS data). Since the PEG linker length is estimated to be 8-9 nm when fully extended, these particle sizes are consistent with functionalized E2.

CD data of the functionalized particles exhibit the spectra of the typical intact E2 protein **nanoparticles** (Figure 3D) [3]. These spectra are characteristic of proteins with a high level of α-helical structure, and confirm that the functionalized particles are correctly folded. Figure 3D shows representative spectra for the **unfunctionalized D381C and the** double-functionalized D381C-AF532-PEG-FA and D381C-DOX-PEG-FA nanoparticles. **This data** further confirms that attachment of foreign molecules inside and outside the scaffold does not disrupt assembly of nanoparticles.

3.3 Folic acid conjugated to protein nanoparticles enhances the uptake in cells expressing FR

To investigate targeting to the folate receptor (FR) by D381C-AF532-PEG-FA, we measured cellular uptake. The FR is a membrane-bound protein and has been reported to be over-expressed at different levels by various carcinoma cells [16-19]. To select cell lines in these investigations, we examined the FR expression level in three cell lines commonly used in FR targeting studies: KB, HeLa, and A549 cells. As shown in Figure 4, FRs were detected in all three cell lines, with both KB and HeLa cells expressing higher levels of FR than A549 cells. These results are consistent with prior reports [19, 20, 22], and we selected KB and A549 cells as FR-positive and FR-negative cell models, respectively.

We first conjugated FA molecules directly to D381C-AF532 through EDC-activated chemical conjugation [29]. However, no uptake difference between D381C-AF532-FA and D381C-AF532 in KB cells was observed, and we hypothesized two possible reasons for this result. First, direct conjugation of FA to the protein nanoparticle surface, without a linker,

may not enable enough flexibility for cell recognition by FR; FA may be bound too close on the surface of the protein nanoparticle, hindering interaction with the folate receptor. Second, nonspecific uptake of E2 protein nanoparticles by the cells may be high, as was previously observed for breast cancer cells [8]. To solve these two problems, we used a PEG linker to attach folic acid to the outer surface of D381C-AF532 (D381C-AF532-PEG-FA). PEG attachment to D381C-AF532 without FA was used as a control (D381C-AF532-PEG). PEGylation is commonly used to modify nanoparticles to modulate cellular and immunological responses [23, 28], and our prior studies showed PEGylation of the E2 nanoparticle reduced cellular uptake at levels correlated to the PEG chain length [8].

We examined the internalization of D381C-AF532-PEG-FA and D381C-AF532-PEG by KB and A549 cells using flow cytometry. Figure 5 shows that uptake of D381C-AF532-PEG-FA is 61.3 ± 1.4 % in KB cells and 16.0 ± 1.2 % in A549 cells, respectively. Therefore, uptake of the nanoparticles with FA is approximately four times greater in cells overexpressing FR than in FR-negative cells. In contrast, uptake of D381C-AF532-PEG (without FA) is 10.2 ± 0.9 % in KB cells and 10.3 ± 1.0 % in A549 cells, indicating comparable baseline uptake in both cell lines when FA is not used as a ligand. This data also shows that the FA moiety conjugated on the D381C-AF532-PEG-FA nanoparticle enhances its uptake approximately six-fold in KB cells, which overexpress the FR.

3.4 Unbound folic acid inhibits uptake of D381C-AF532-PEG-FA in KB cells

To verify that the enhanced cellular uptake of folate-displayed nanoparticles is specifically mediated by the interaction between FR and FA, we performed an inhibition assay by pre-incubating cells with 1 mM unbound FA. Figure 6 shows that uptake of D381C-AF532-PEG-FA in KB cells, with and without pre-treatment with FA, is 16.6 ± 0.8% and 61.3 ± 1.4 % respectively. Thus, folic acid inhibits the uptake of D381C-AF532-PEG-FA in cells overexpressing the FR by approximately four-fold. However, in A549 cells, uptake of D381C-AF532-PEG-FA with and without FA treatment is 16.0 ± 0.6 % and 16.0 ± 1.2 %, respectively, indicating no difference in nanoparticles uptake when a marginal level of FR is expressed on the cell surface. These results also show that free FA can inhibit the uptake of D381C-AF532-PEG-FA in KB cells, reducing internalization down to a level comparable to FR-negative cells. These results further confirm the role of FA in the internalization of D381C-AF532-PEG-FA, and suggest that nanoparticles are taken up through folate receptor-mediated endocytosis [17, 31].

Our FA results are consistent with previously-reported studies using other nanoparticulate systems, including viral capsids [28, 32], polymer-based micelles [33], and quantum dots [22]. Increased binding and internalization of FA-displaying macromolecular systems have been consistently observed for FR-bearing cells. Furthermore, uptake is also FA-dependent, as nanoparticle internalization is reduced when FR on the cells is saturated by folic acid. Therefore, our results demonstrate our ability to modulate cellular internalization by appropriately functionalizing the external surface of the E2 nanoparticle surface.

3.5 CLSM shows different intracellular distribution of D381C-AF532-PEG-FA and D381C-AF532-PEG in KB cells

We visualized the intracellular distribution of D381C-AF532-PEG-FA and D381C-AF532-PEG in KB cells by CLSM. The cell nuclei are stained blue (Figure 7A), the AF532-encapsulated D381C is green (Figure 7B), and the overlay are also presented (Figure 7C). Greater fluorescence intensities were observed in cells incubated with D381C-AF532-PEG-FA than with D381C-AF532-PEG (Figure 7B), and indicates that KB cells take up more nanoparticles that are coated with FA, likely through folate receptor-mediated endocytosis. This result is consistent with our flow cytometry results (Figure 5), and the data together suggests D381C-AF532-PEG-FA and D381C-AF532-PEG are taken up by KB cells through different mechanisms and at different rates. The analogous experiment in A549 cells did not yield observable intracellular fluorescence intensity differences between the two different nanoparticles. Uptake of D381C-AF532-PEG-FA and D381C-AF532-PEG in A549 cells and D381C-AF532-PEG in KB cells are most likely through non-specific endocytosis, since the particle sizes are within the optimal range for endocytosis [9, 10].

Our results are consistent with other studies which showed different intracellular distribution of FA functionalized particles and non-functionalized particles in KB cells as well and are also consistent with uptake of D381C-AF532-PEG-FA in KB cells through the folate-specific receptor-mediated endocytosis pathway [28, 34]. Although the existence of folate receptor-mediated endocytosis has been well established [16, 29, 31], the specifics of this endocytosis mechanism are unclear. The variety of different proposed mechanisms may be that divergent mechanisms indeed are observed based on experimental variations; for example, internalization differences have been reported depending on the valency of the folate conjugates [18, 29]. In spite of these discrepancies, it is widely accepted that folate receptor-mediated endocytosis commences with FA binding to FR [17, 31].

3.6 FA-functionalized, DOX-encapsulating nanoparticles exhibit cytotoxicity to cells

To investigate the effects of attaching FA to DOX-loaded nanoparticles, we incubated nanoparticles with KB and A549 cells and measured cytotoxicities. Dose-response curves for KB cells incubated for 48 hrs with D381C-DOX-PEG-FA, D381C-DOX-PEG, D381C-DOX, and free DOX yielded IC_{50} values of 1.3 ± 0.04 μM, 0.9 ± 0.1 μM, 1.3 ± 0.3 μM and 0.2 ± 0.001 μM, respectively. IC_{50} values for D381C-DOX-PEG-FA, D381C-DOX-PEG, D381C-DOX and DOX in A549 cells were 1.3 ± 0.2 μM, 0.9 ± 0.5 μM, 1.6 ± 0.3 μM and 0.4 ± 0.2 μM, respectively. Results show that all nanoparticles were cytotoxic towards cells and that therefore DOX is delivered and released by the D381C particle. As with prior results utilizing DOXO-EMCH for conjugation [5, 24, 35], the IC_{50} for free DOX is lower than that for macromolecule-bound DOX, which is likely due to different uptake mechanisms between free and protein-bound DOX [5, 36].

Given our cell uptake results (Figures 5 & 6), we initially expected that E2 nanoparticles displaying the FA targeting ligand (D381C-DOX-PEG-FA) would be more cytotoxic (i.e., lower IC_{50} values) than D381C-DOX-PEG in the FR-positive KB cells. Surprisingly, we did not observe significant differences in cytotoxicity between D381C-DOX-PEG-FA and D381C-DOX-PEG in either KB or A549 cells. While many *in vitro* studies have indeed

observed an increase in drug cytotoxicity due to FR-targeting, investigations utilizing acid-responsive drug conjugates [35] or lysosomal enzyme-responding macromolecules [17] have also observed no effect of FA.

This observation can potentially be explained by different relative kinetic rates in the *in vitro* assays [35]. Our flow cytometry results show a significant uptake of folate-conjugated nanoparticles via FR within relatively short times (*i.e.* 0.5 hr). In contrast, the acid-cleavable hydrazone bond that attaches DOX to the nanoparticle is active at much slower rates for hydrolysis (50% DOX release from D381C after 24 hr at pH 5 [5]), and therefore significant cytotoxicity was observed in cells after at least 48 hr incubation. These longer incubation times, however, allow the uptake of all nanoparticles through non-specific internalization, thereby minimizing the uptake and cytotoxicity differences due to FA targeting. Indeed, this hypothesis is supported by the close range of IC_{50} values for D381C-DOX, D381C-DOX-PEG, and D381C-DOX-PEG-FA. Furthermore, studies have reported that the efficacy of doxorubicin-carrier complexes can be vastly different between *in vitro* and *in vivo* studies. DOXO-EMCH bound to human serum albumin shows comparable *in vitro* IC_{50} values (to IC_{50} for D381C-DOX, D381C-DOX-PEG, and D381C-DOX-PEG-FA), but it was significantly more efficacious in tumor-bearing *in vivo* murine models. This albumin-binding DOXO-EMCH is now undergoing clinical trials [37]. These reasons suggest that *in vivo* studies and the kinetics of biodistribution, cellular uptake, and drug release will be important for assessing the therapeutic value of our acid-sensitive DOX nanoparticle.

4. CONCLUSIONS

We have successfully fabricated protein-based E2 nanoparticles which were functionalized both internally (with drug and imaging molecules) and externally (with tumor-targeting ligands) to yield bi-functional nanoparticles. These functionalized particles remained intact, yielding sizes consistent with expected values. Surface conjugation of FA enhanced the cellular uptake six times relative to the non-targeting control nanoparticles in high-FR expressing KB cells, but was not significantly increased in A549 cells with minimal FR. This FA-FR specific interaction was confirmed by inhibition assays with free FA, suggesting that our proteins with FA are taken up by folate receptor-mediated endocytosis. CLSM imaging showed different intracellular intensities and distribution of D381C-AF532-PEG-FA and D381C-AF532-PEG. Additionally, the E2 protein nanoparticles encapsulating DOX exhibited cytotoxicity to tumor cells. Overall, we demonstrate the feasibility of using recombinant biofabrication methods to produce well-defined protein-based nanoparticles with different functionalities that have the potential as novel drug delivery systems for tumor targeting.

Acknowledgments

REFERENCES

1. Uchida M, Klem MT, Allen M, Suci P, Flenniken M, Gillitzer E, Varpness Z, Liepold LO, Young M, Douglas T. Biological Containers: Protein Cages as Multifunctional Nanoplatforms. Adv Mater. 2007; 19:1025–1042.

2. DiMarco RL, Heilshorn SC. Multifunctional Materials through Modular Protein Engineering. Adv Mater. 2012; 24:3923–3940. [PubMed: 22730248]

3. Dalmau M, Lim S, Chen HC, Ruiz C, Wang S-W. Thermostability and molecular encapsulation within an engineered caged protein scaffold. Biotechnology and Bioengineering. 2008; 101:654–664. [PubMed: 18814295]

4. Allen MD, Perham RN. The catalytic domain of dihydrolipoyl acetyltransferase from the pyruvate dehydrogenase multienzyme complex of *Bacillus stearothermophilus*: Expression, purification and reversible denaturation. FEBS Letters. 1997; 413:339–343. [PubMed: 9280309]

5. Ren D, Kratz F, Wang S-W. Protein Nanocapsules Containing Doxorubicin as a pH-Responsive Delivery System. Small. 2011; 7:1051–1060. [PubMed: 21456086]

6. Ren D, Dalmau M, Randall A, Shindel MM, Baldi P, Wang S-W. Biomimetic Design of Protein Nanomaterials for Hydrophobic Molecular Transport. Advanced Functional Materials. 2012; 22:3170–3180. [PubMed: 23526705]

7. Dalmau M, Lim S, Wang S-W. Design of a pH-Dependent Molecular Switch in a Caged Protein Platform. Nano Letters. 2008; 9:160–166. [PubMed: 19113890]

8. Molino NM, Bilotkach K, Fraser DA, Ren D, Wang S-W. Complement Activation and Cell Uptake Responses Toward Polymer-Functionalized Protein Nanocapsules. Biomacromolecules. 2012; 13:974–981. [PubMed: 22416762]

9. Jiang W, Kim BYS, Rutka JT, Chan WCW. Nanoparticle-mediated cellular response is size-dependent. Nat Nano. 2008; 3:145–150.

10. Chithrani BD, Ghazani AA, Chan WCW. Determining the Size and Shape Dependence of Gold Nanoparticle Uptake into Mammalian Cells. Nano Letters. 2006; 6:662–668. [PubMed: 16608261]

11. Greish K. Enhanced permeability and retention of macromolecular drugs in solid tumors: A royal gate for targeted anticancer nanomedicines. Journal of Drug Targeting. 2007; 15:457–464. [PubMed: 17671892]

12. Petros RA, DeSimone JM. Strategies in the design of nanoparticles for therapeutic applications. Nat Rev Drug Discov. 2010; 9:615–627. [PubMed: 20616808]

13. Ruoslahti E, Bhatia SN, Sailor MJ. Targeting of drugs and nanoparticles to tumors. The Journal of Cell Biology. 2009; 188:759–768. [PubMed: 20231381]

14. Cheng Z, Al Zaki A, Hui JZ, Muzykantov VR, Tsourkas A. Multifunctional Nanoparticles: Cost Versus Benefit of Adding Targeting and Imaging Capabilities. Science. 2012; 338:903–910. [PubMed: 23161990]

15. Mahon E, Salvati A, Baldelli Bombelli F, Lynch I, Dawson KA. Designing the nanoparticle-biomolecule interface for "targeting and therapeutic delivery". Journal of Controlled Release. 2012; 161:164–174. [PubMed: 22516097]

16. Sudimack J, Lee RJ. Targeted drug delivery via the folate receptor. Advanced Drug Delivery Reviews. 2000; 41:147–162. [PubMed: 10699311]

17. Lu Y, Low PS. Folate-mediated delivery of macromolecular anticancer therapeutic agents. Advanced Drug Delivery Reviews. 2012; 64(Supplement):342–352.

18. Low PS, Kularatne SA. Folate-targeted therapeutic and imaging agents for cancer. Current Opinion in Chemical Biology. 2009; 13:256–262. [PubMed: 19419901]

19. Parker N, Turk MJ, Westrick E, Lewis JD, Low PS, Leamon CP. Folate receptor expression in carcinomas and normal tissues determined by a quantitative radioligand binding assay. Analytical Biochemistry. 2005; 338:284–293. [PubMed: 15745749]

20. Abu Ajaj K, El-Abadla N, Welker P, Azab S, Zeisig R, Fichtner I, Kratz F. Comparative evaluation of the biological properties of reducible and acid-sensitive folate prodrugs of a highly potent doxorubicin derivative. European Journal of Cancer. 2011; 48:2054–2065. [PubMed: 21937219]

21. Hilgenbrink AR, Low PS. Folate receptor-mediated drug targeting: From therapeutics to diagnostics. Journal of Pharmaceutical Sciences. 2005; 94:2135–2146. [PubMed: 16136558]

22. Bharali DJ, Lucey DW, Jayakumar H, Pudavar HE, Prasad PN. Folate-Receptor-Mediated Delivery of InP Quantum Dots for Bioimaging Using Confocal and Two-Photon Microscopy. Journal of the American Chemical Society. 2005; 127:11364–11371. [PubMed: 16089466]

23. Jokerst JV, Lobovkina T, Zare RN, Gambhir SS. Nanoparticle PEGylation for imaging and therapy. Nanomedicine : the official journal of the American Academy of Nanomedicine. 2011; 6:715–728.

24. Kratz F, Warnecke A, Scheuermann K, Stockmar C, Schwab J, Lazar P, Drückes P, Esser N, Drevs J, Rognan D, Bissantz C, Hinderling C, Folkers G, Fichtner I, Unger C. Probing the Cysteine-34 Position of Endogenous Serum Albumin with Thiol-Binding Doxorubicin Derivatives. Improved Efficacy of an Acid-Sensitive Doxorubicin Derivative with Specific Albumin-Binding Properties Compared to That of the Parent Compound. Journal of Medicinal Chemistry. 2002; 45:5523–5533. [PubMed: 12459020]

25. Stella B, Arpicco S, Peracchia MT, Desmaele D, Hoebeke J, Renoir M, D'Angelo J, Cattel L, Couvreur P. Design of folic acid-conjugated nanoparticles for drug targeting. Journal of Pharmaceutical Sciences. 2000; 89:1452–1464. [PubMed: 11015690]

26. Paulos CM, Reddy JA, Leamon CP, Turk MJ, Low PS. Ligand Binding and Kinetics of Folate Receptor Recycling in Vivo: Impact on Receptor-Mediated Drug Delivery. Molecular Pharmacology. 2004; 66:1406–1414. [PubMed: 15371560]

27. Wang S-W, Monagle J, McNulty C, Putnam D, Chen H. Determination of P- glycoprotein inhibition by excipients and their combinations using an integrated high-throughput process. Journal of Pharmaceutical Sciences. 2004; 93:2755–2767. [PubMed: 15389668]

28. Destito G, Yeh R, Rae CS, Finn MG, Manchester M. Folic Acid-Mediated Targeting of Cowpea Mosaic Virus Particles to Tumor Cells. Chemistry & Biology. 2007; 14:1152–1162. [PubMed: 17961827]

29. Delgado, C.; Lee, R.; Low, P. Drug Targeting. Humana Press; 2000. Folate as a Targeting Device for Proteins Utilizing Folate Receptor-Mediated Endocytosis; p. 69-76.

30. Zheng CY, Ma G, Su Z. Native PAGE eliminates the problem of PEG–SDS interaction in SDS-PAGE and provides an alternative to HPLC in characterization of protein PEGylation. Electrophoresis. 2007; 28:2801–2807. [PubMed: 17702059]

31. Xu S, Olenyuk BZ, Okamoto CT, Hamm-Alvarez SF. Targeting receptor- mediated endocytotic pathways with nanoparticles: Rationale and advances. Advanced Drug Delivery Reviews. 2013; 65:121–138. [PubMed: 23026636]

32. Ren Y, Wong SM, Lim L-Y. Folic Acid-Conjugated Protein Cages of a Plant Virus: A Novel Delivery Platform for Doxorubicin. Bioconjugate Chemistry. 2007; 18:836–843. [PubMed: 17407258]

33. Wang Y, Yu L, Han L, Sha X, Fang X. Difunctional Pluronic copolymer micelles for paclitaxel delivery: Synergistic effect of folate-mediated targeting and Pluronic-mediated overcoming multidrug resistance in tumor cell lines. International Journal of Pharmaceutics. 2007; 337:63–73. [PubMed: 17289311]

34. Yoo HS, Park TG. Folate-receptor-targeted delivery of doxorubicin nano- aggregates stabilized by doxorubicin-PEG-folate conjugate. Journal of Controlled Release. 2004; 100:247–256. [PubMed: 15544872]

35. Scomparin A, Salmaso S, Bersani S, Satchi-Fainaro R, Caliceti P. Novel folated and non-folated pullulan bioconjugates for anticancer drug delivery. Eur J Pharm Sci. 2011; 42:547–558. [PubMed: 21371555]

36. Speelmans G, Staffhorst RWHM, de Kruijff B, de Wolf FA. Transport Studies of Doxorubicin in Model Membranes Indicate a Difference in Passive Diffusion across and Binding at the Outer and Inner Leaflet of the Plasma Membrane. Biochemistry. 1994; 33:13761–13768. [PubMed: 7947787]

37. Kratz F. DOXO-EMCH (INNO-206): the first albumin-binding prodrug of doxorubicin to enter clinical trials. Expert Opin Inv Drug. 2007; 16:855–866.

Highlights

- We fabricated biomimetic protein-based nanoparticles with both molecular encapsulation and cell-targeting capabilities using recombinant technology and chemical synthesis.

- Functionalization of the protein nanoparticles' external surface with folic acid increased their cellular uptake into cancer cells that overexpressed folate receptors.

- Nanoparticles demonstrated acid-responsive drug release and were cytotoxic to cancer cells.

- Our investigation demonstrates the potential of using biofabrication strategies to generate functional nanomaterials.

(A)

(B)

Alexa Fluor 532 C$_5$ maleimide (AF532)

(6-Maleimidocaproyl) hydrazone of doxorubicin
(DOXO-EMCH)
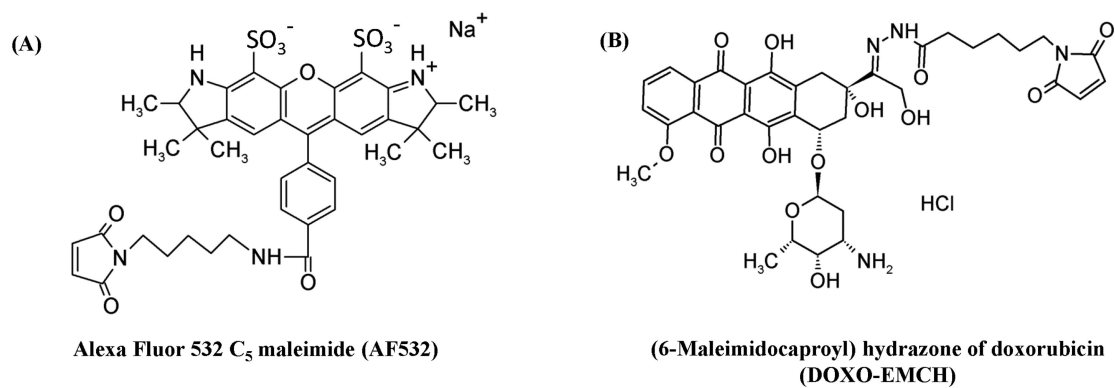
Figure 1.
Chemical structures of (A) Alexa Fluor 532 C$_5$ maleimide and (B) DOXO-EMCH.
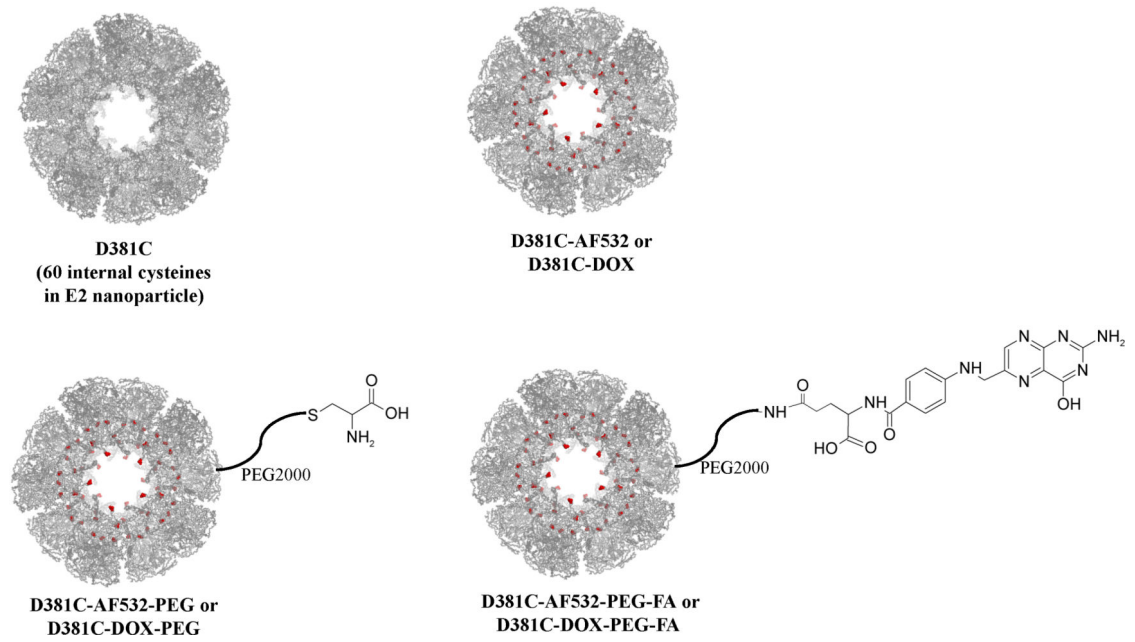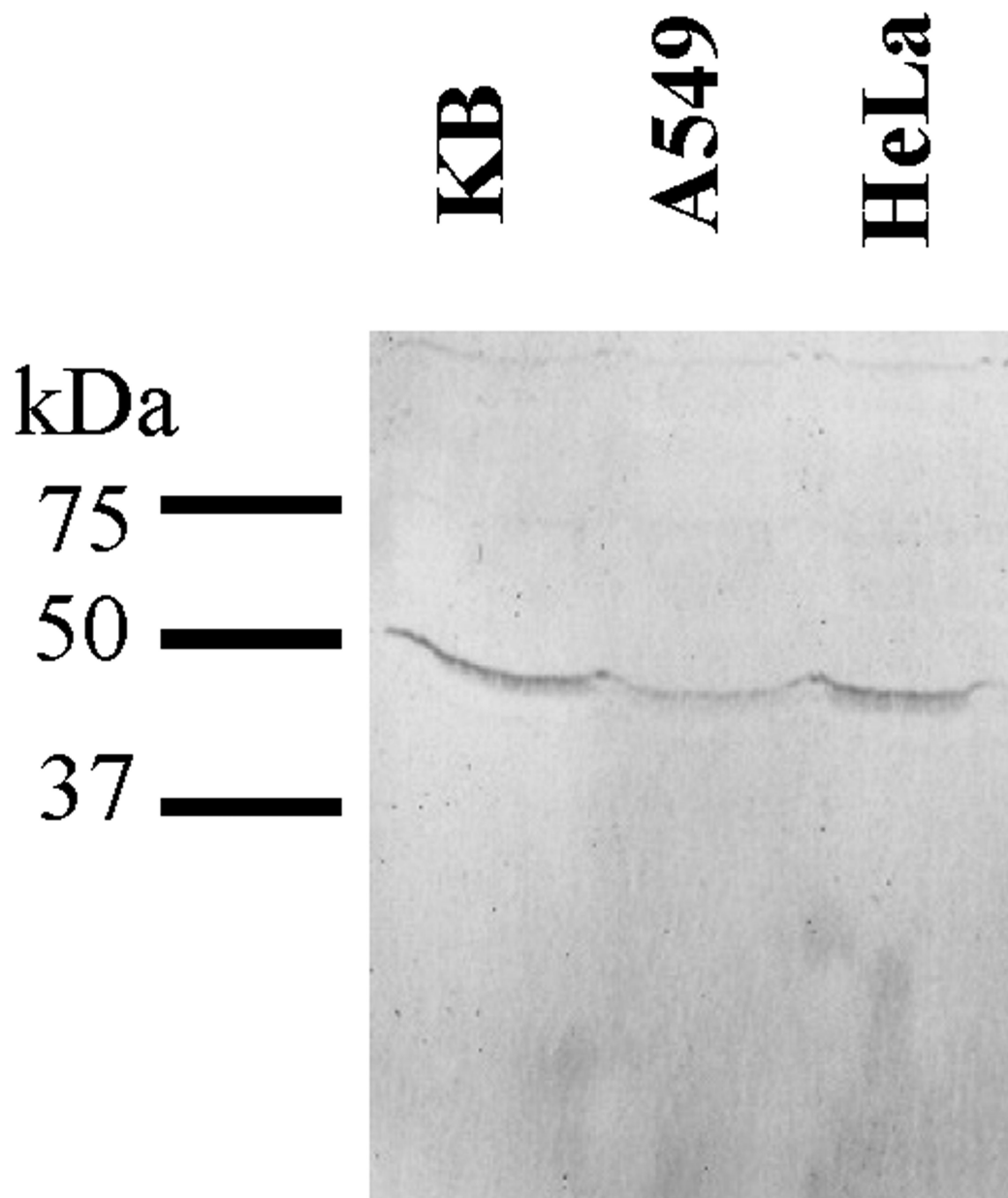
Figure 2.
Summary of functionalized protein nanoparticles.
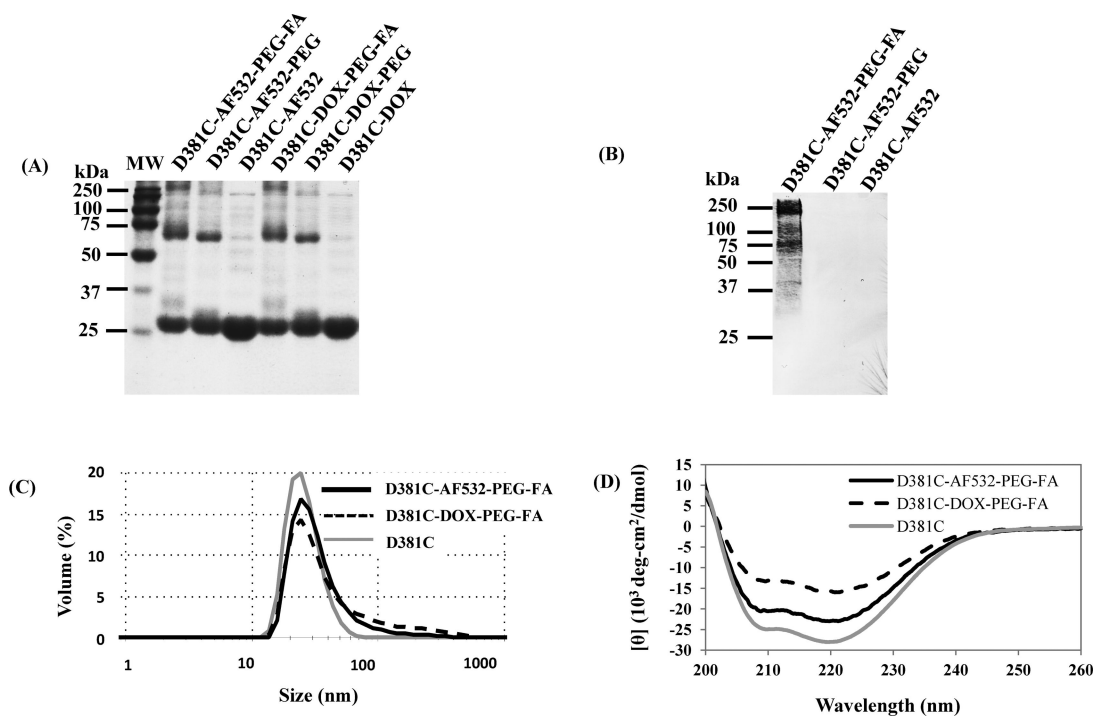
Figure 3.
Representative images of nanoparticle characterization shows conjugation of functional groups and correct assembly. (A) SDS-PAGE of functionalized nanoparticles; (B) Western blot for folic acid conjugation; (C) DLS shows the diameter size of nanoparticles; (D) CD wavelength spectra confirms secondary structure of protein nanoparticles.
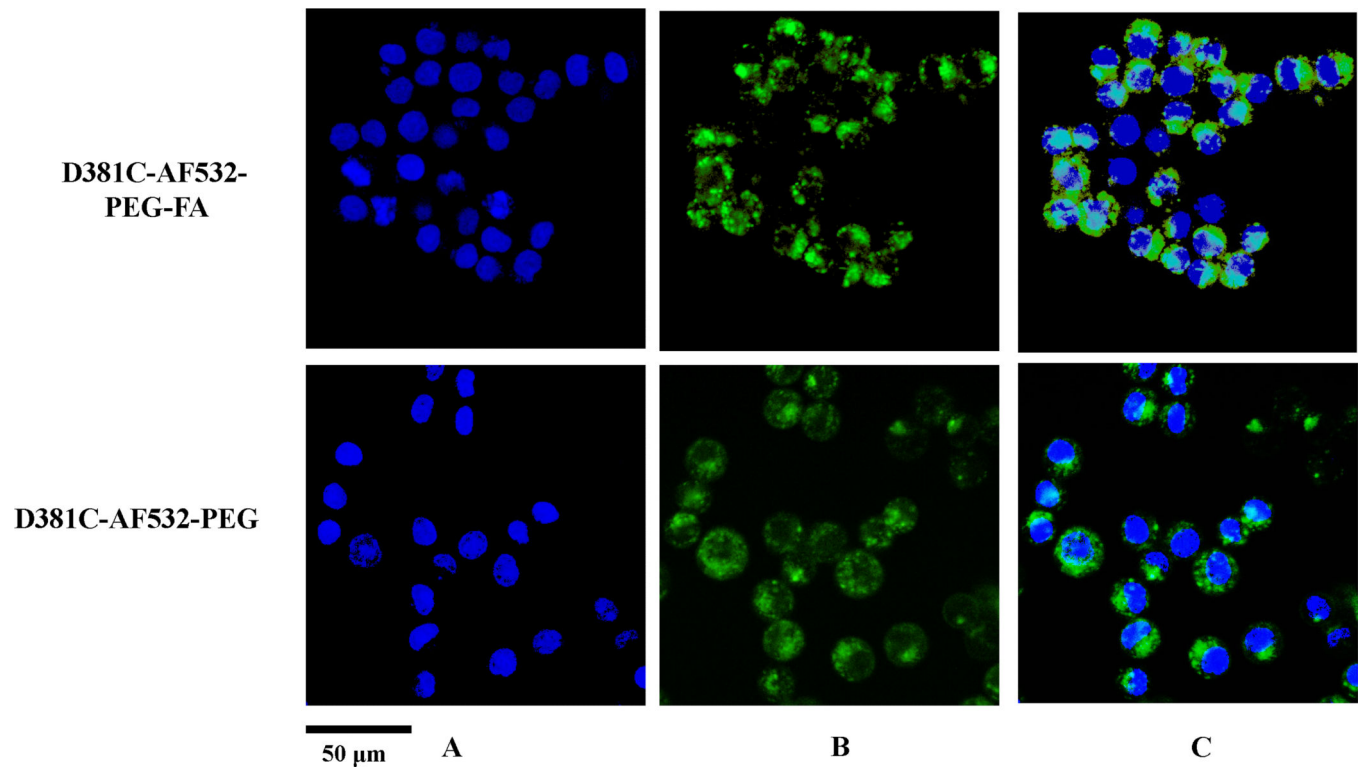
Figure 4.
Western blot shows higher folate receptor expression in KB and HeLa cells than in A549 cells.
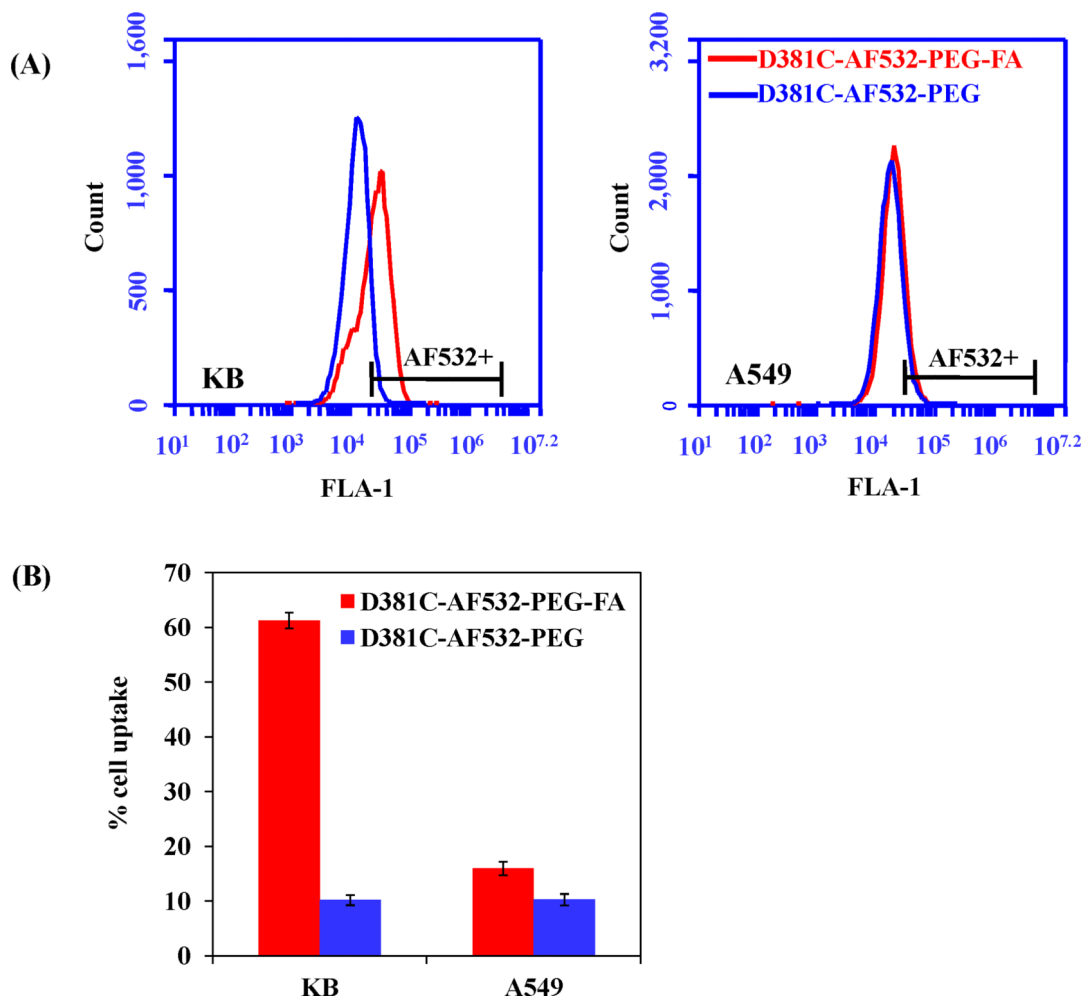
Figure 5.
Flow cytometry data measuring uptake of D381C-AF532-PEG-FA and D381C-AF532-PEG in KB and A549 cells at 37 °C. (A) Histograms of cell populations. (B) Percentage of cells which have internalized fluorescent protein nanoparticles.
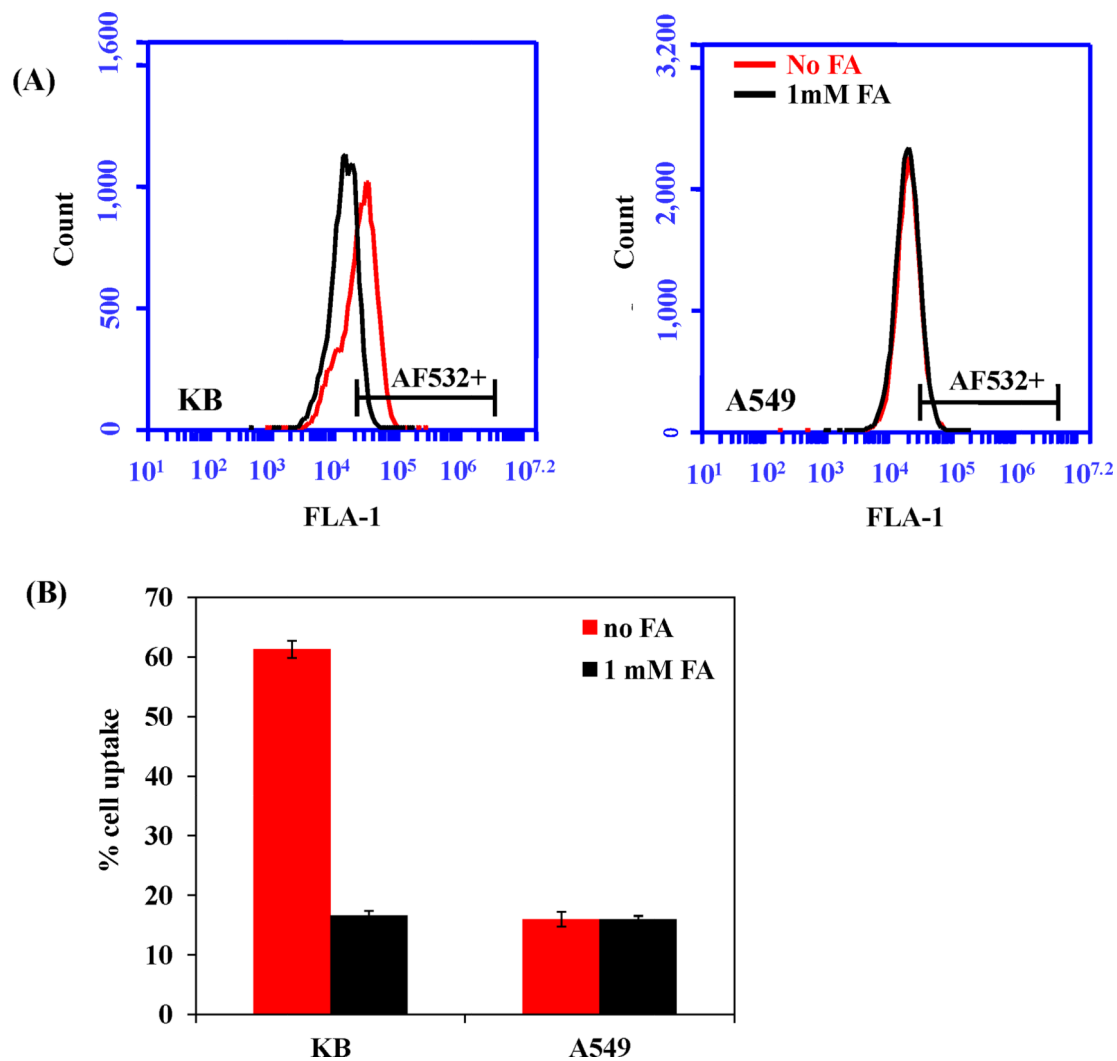
Figure 6.
Uptake of D381C-AF532-PEG-FA in KB and A549 cells at 37 °C, with and without pre-incubation of free folic acid. (A) Flow cytometry histograms of cell populations. (B) Percentage of cells which have internalized fluorescent protein nanoparticles.

Figure 7.
Confocal laser scanning microscopy images of KB cells incubated with D381C-AF532-PEG-FA (top) and D381C-AF532-PEG (bottom). (A) Nuclei were stained blue with Hoechst 33342, (B) protein nanoparticles were green with AF532M, and (C) overlay of the two is shown. Scale bar is 50 μm.

Table 1

Characterization summary of functionalized protein nanoparticles

	No. of AF532 or DOX molecules per particle	No. of FA molecules per particle	Average particle diameter (nm)
D381C-AF532-PEG-FA	73.6 ± 11.7	35.1 ± 6.3	37.6 ± 4.3
D381C-AF532-PEG	72.3 ± 12.9	N/A	35.0 ± 4.5
D381C-AF532	68.0 ± 4.9	N/A	30.6 ± 0.4 [*]
D381C-DOX-PEG-FA	82.2 ± 5.1	27.9 ± 0.4	42.8 ± 13.4
D381C-DOX-PEG	80.1 ± 3.0	N/A	48.4 ± 5.6
D381C-DOX	99.3 ± 10.1 ^	N/A	33.8 ± 4.1 [*]

[*]
value obtained from Ren *et al.* [5]